



<sup>1</sup> Robert POSPICHAL, <sup>2</sup> Gerhard LIEDL

## LASER ABLATION OF POLYETHYLENE TEREPHTHALATE NON-WOVEN FABRICS

<sup>1,2</sup> Vienna University of Technology, Institute for Production Engineering and Laser Technology,  
Gusshausstrasse 30, Vienna, AUSTRIA

**Abstract:** Importance of product-lifecycle-management (PLM) increased in production engineering during the last years. Environmental as well as economic constraints account for intensified efforts in recycling and substitution of non-environmental friendly products. For example, Polyurethane (PU) foams should be replaced with non-woven fabrics. Unfortunately, unlike foams, such non-woven fabrics exhibit limited possibilities in molding operations. Material removal by means of laser processing offers a possibility in a partial replacement of difficult moldings. Experiments of CO<sub>2</sub>-laser processing of polyethylene terephthalate (PET) are presented. Laser parameters like beam shape, intensity distribution and process gases have been varied to optimise results.

**Keywords:** laser processing, non-woven fabrics, beam forming, recycling

### 1. INTRODUCTION

The most commonly used material for foam mouldings is Polyurethane (PU). Main advantages of this material are its elasticity, its reset force after deformation, as well as its endurance strength and form stability. It is also breathable and allows water transportation. Very thin moldings with complex geometry are possible [1].

Main disadvantage of PU foams are their very limited recycling abilities. In most cases recycling is not efficient under an economical point of view [2]. Due to changes in regulatory framework (Directive 2000/53/EC) producers are forced to increase reuse and recovery of their goods [3].

One possibility to do so is the application of non-woven fabrics instead of foams. While they are challenging in production, they are beneficial in recycling, as the non-woven fabrics can be made out of thermoplastic fibres, which have tremendous advantages in recycling.

The feasibility of the production process to make moldings during the forming process is very limited. Building complex geometries during the forming operation would cause inhomogeneity in the final product. A subsequent laser ablation or cutting process can solve this problem.

Aim of the presented work was to ablate box-shaped moldings with a more or less flat surface into a given polyethylene terephthalate (PET) non-woven fabric with an industrial CO<sub>2</sub> Laser. Main problems are the formation of drops and the shape of the resulting cross section.

### 2. MATERIALS

Materials used for experiments presented here are PET non-woven fabrics, which have been provided by our industrial partner. Non-woven fabric production was done in the dry fleece process, bonding was done thermal. Due to a non-disclosure agreement no textile specific data will be mentioned in this paper.

Density and thermodynamic material data will be needed for further calculations. The density has been measured and calculated with a mean value out of five samples. Enthalpy of fusion and evaporation can be found at Bäuerle [4]. According to Schuöcker [5], optical absorption coefficient

for plastics can be assumed with 1 at 10.6  $\mu\text{m}$  wavelength. Although the used material does not exhibit a closed surface and radiation therefore can transmit a certain volume into the bulk of the material, material seems thick enough, to absorb the complete radiation. The assumed absorption coefficient 1 seems correct, as long do not want to explain surface near interactions. Melting and decomposition temperature can be found at Kroschwitz [6].

Table 1: Material data [4, 5, 6]

density [kg/m <sup>3</sup> ]	Hm [J/kg]	Hv [J/kg]	cp [J/kgK]	Tm °K	Tvap °K	A
35 - 55	17	970	3150	541,15	556,15 - 579,15	1

Real material properties will of course differ from values found in literature, but the error seems adequate for the presented rough calculations.

### 3. THEORETICAL CONSIDERATIONS

Optical Power  $P_L$  required for laser ablation processes can be estimated with the equation:

$$A * P_L = P_{\text{proc}} + P_{\text{chem}} + P_{\text{cond}} + P_{\text{conv}} \quad (1)$$

With A as the absorption coefficient. In most laser applications heat losses due to convection  $P_{\text{conv}}$  or heat conduction  $P_{\text{cond}}$  can be neglected, as well as chemical reactions  $P_{\text{chem}}$ . This work will show that this assumption may not be appropriate in this case. Losses will be summarised in  $P_{\text{loss}}$ .

The power needed to evaporate a certain volume in a given time can be calculated as follows [5]:

$$P_{\text{proc}} = v * w_s * s * Q * (c_{\text{solid}} * (T_m - T_0) + h_m + c_{\text{liquid}} * (T_{\text{vap}} - T_m) + h_{\text{vap}}) \quad (2)$$

Where v is the propagation speed,  $w_s$  is the diameter of the evaporated area, c is the specific heat capacity and h is the enthalpy of fusion respectively evaporation.

The theoretic area cross-section follows with

$$A_{\text{cross}} = w_s * s = \frac{A * P_L - P_{\text{loss}}}{v * (c_{\text{solid}} * (T_m - T_0) + h_m + c_{\text{liquid}} * (T_{\text{vap}} - T_m) + h_{\text{vap}})} \quad (3)$$

### 4. EXPERIMENTAL SETUP

Two different CO<sub>2</sub>-laser systems have been used for the experiments, an EMCO LS140 and an OPL2000. Absorption coefficients for plastics and the fact that CO<sub>2</sub>-lasers have a long history of usage in industrial applications are main advantages for the intended application.

Table 2: Parameters of laser systems used for experiments

	Max. optical Power [W]	Wavelength h [ $\mu\text{m}$ ]	Raw beam diameter [mm]	Beam divergence (full angle) [mrad]	Polarisation
EMCO LS140	200	10.6	12	2	Not polarised
OPL 2000	2000	10.6	13	2	Vertical, linear

To achieve box-shaped mouldings, the laser beam divergence should be kept as low as possible. A lens with a relatively long focal length of 200 mm has been used for first experiments. The waist of the focused beam in dependency of the position z can easily be calculated [7]:

$$w(z) = w_0 \sqrt{1 + \left(\frac{BPP_{\text{real}} * z}{w_0^2}\right)^2} \quad (4)$$

Whereas  $w_0$  is the focal waist,  $BPP_{\text{real}} = \theta * w_0$  is the real beam parameter product and z is the distance in propagation direction. According to the equation above the resulting beam diameter between 100 mm and 130 mm above the focal point varies between 8 and 6.5 mm.

Results of the first series of experiments indicate that the intensity distribution of the laser beam influences the shape of the moulding strongly. As a consequence, a beam homogenization unit has been designed.

#### 4.1. Beam homogenization

Since the beam mode influences the ability how a laser can be focused, most cutting lasers are operated as close as possible to the fundamental TEM<sub>00</sub> mode. Such an intensity distribution can be focused to the smallest possible focus size and is beneficial for the overall efficiency of a cutting laser system.

On the other hand, laser surface treatment requires larger spot sizes to process larger areas within reasonable time and a more or less homogeneous intensity distribution. Even though the beam size can be enlarged by defocusing, beam homogenization requires additional efforts.

For the sake of simplicity we used a kaleidoscope for beam homogenization. A kaleidoscope uses multiple reflections inside a rectangular shaped beam guide for homogenization. Depending on the surface properties, power loss inside a kaleidoscopic beam homogenizer can be quite large which in turn causes a necessity for cooling.

The dimensions of the kaleidoscope as well as the lenses used for focusing the laser beam are important design parameters for beam homogenization. For optimization we used the matrix method for description of the propagation of the beam through the optical system.

In the paraxial approximation, a ray of light can be described by its position from the optical axis and its angle. Propagation through free space alters the distance but not the angle of the ray to the optical axis. Optical elements, like lenses or mirrors alter the direction of beam propagation. The effects of such optical elements can be described by means of a 2x2 matrix which modifies the ray vector [8].

In the following a description of the transfer matrix of a kaleidoscope as shown in figure 1 is given briefly.

The overall length of the kaleidoscope is  $L$  and its opening has a width  $d$  and a quadratic cross section.

According to figure 1 an incoming ray enters the kaleidoscope at a certain position  $y$  and an inclination

$\phi$ . After propagation towards the first surface (region 1), the beam is reflected in region 2. Depending on the overall length of the kaleidoscope and the angle of the incoming beam(s), the beam pattern in region 2 has to be repeated several times. In region 3, the beam is reflected again and enters region 4 or the beam leaves the kaleidoscope. Depending on the number of reflections inside the kaleidoscope the beam leaves the unit in the same direction as the incoming beam or inverted along the optical axis of the system.

In region 1, the beam propagates a length  $l_1$  until it hits the first reflecting surface. The transfer matrix reads as follows

$$\begin{bmatrix} 1 & l_1 \\ 0 & 1 \end{bmatrix} = \begin{bmatrix} 1 & (d/2 - y) / \tan \phi \\ 0 & 1 \end{bmatrix} = M_1 \quad (5)$$

In region 2, the beam is reflected towards the opposite wall. After propagation of a certain distance  $l_2$  the beam is reflected towards the opposite surface and after propagation of an additional distance  $l_2$  the beam hits the first reflecting surface again. Irrespective of the number of repetitions, the beam is reflected in the same direction as after the first reflection. As a consequence, the sum of reflections in region 2 can be treated just as the first reflection, repeated  $N$  times. Beam propagation along the distance  $2 \cdot l_2$  can safely be neglected and the beam transfer matrix reads as:

$$\begin{bmatrix} 1 & 0 \\ 0 & 1 \end{bmatrix}^N = M_2 \quad (6)$$

Beam transfer in regions 3 and 4 depend on the remaining length of the optical element. At an odd number of reflections inside the element, the beam leaves the kaleidoscope in the same direction as the incoming beam but with an inverted position, at an even number of reflections the beam position remains unchanged and the direction is inverted in relation to the optical axis.

The number of reflections depends on the dimensions of the kaleidoscope and the properties of the incoming beam. With  $l_2 = d / \tan \phi$ , the number of reflections  $R$  can be calculated by an integer division of the remaining length of the kaleidoscope by the length  $l_2$ ,  $R = \text{int}(\frac{L - l_1}{l_2})$ . If we define the

next beam transfer matrix, we have to distinguish between two possibilities. As mentioned before, the first possibility transfers the beam in such a way that the inclination of the beam leaving the kaleidoscope is identical to the incoming beam. The position is inverted from the first reflecting

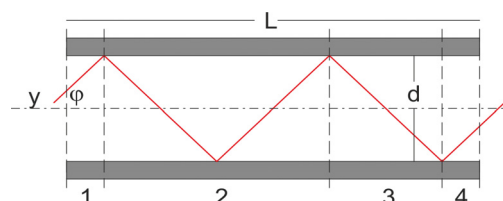


Figure 1: Light path through a kaleidoscope with length  $L$  and opening width  $d$

surface to the second surface which gives a beam transfer matrix of  $\begin{bmatrix} -1 & 0 \\ 0 & 1 \end{bmatrix}$ . In the second case the beam position remains unchanged and the beam direction is inverted, which results in a beam transfer matrix of  $\begin{bmatrix} 1 & 0 \\ 0 & -1 \end{bmatrix}$ .

By combining both beam transfer matrices, we can define a matrix for region 3

$$\begin{bmatrix} -1^R & 0 \\ 0 & -1^{(R+1)} \end{bmatrix} = (-1)^R \begin{bmatrix} 1 & 0 \\ 0 & -1 \end{bmatrix} = M_3 \quad (7)$$

The remaining beam path inside the kaleidoscope can be treated as a linear translation along a distance  $l_4$  and the beam transfer matrix is defined as  $\begin{bmatrix} 1 & l_4 \\ 0 & 1 \end{bmatrix} = M_4$ .

The distance  $l_4$  can be determined as  $l_4 = L - R \cdot l_2 - l_1$  and depends on the dimensions of the kaleidoscope and the beam parameters. Now the overall transfer matrix can be defined:

$$M_R = M_4 \cdot M_3 \cdot M_2 \cdot M_1 = (-1)^R \begin{bmatrix} 1 & l_4 \\ 0 & 1 \end{bmatrix} \cdot \begin{bmatrix} 1 & 0 \\ 0 & -1 \end{bmatrix} \cdot \begin{bmatrix} 1 & 0 \\ 0 & 1 \end{bmatrix} \cdot \begin{bmatrix} 1 & l_1 \\ 0 & 1 \end{bmatrix} = (-1)^R \begin{bmatrix} 1 & l_1 - l_4 \\ 0 & -1 \end{bmatrix} \quad (8)$$

An incoming beam with a position  $y$  and an inclination  $\phi$  at the entrance of the optical unit is transferred with the transfer matrix to a beam with coordinates  $y'$  and  $\phi'$ . For a complete treatment of such an optical element, the beam transfer matrices of focusing elements prior and after the kaleidoscope have to be taken into account. The following transfer matrix describes a lens  $f_1$ , followed by propagation  $T_1$ . Now the beam is transferred by the kaleidoscope  $M_K$  followed by free space propagation  $T_2$ . The last lens  $f_2$  gathers the rays and after propagation  $T_3$  the beam hits the surface of the sample.

$$M_{Total} = (-1)^R \begin{bmatrix} 1 & T_3 \\ 0 & 1 \end{bmatrix} \cdot \begin{bmatrix} 1 & 0 \\ -\frac{1}{f_2} & 1 \end{bmatrix} \cdot \begin{bmatrix} 1 & T_2 \\ 0 & 1 \end{bmatrix} \cdot \begin{bmatrix} 1 & l_1 - l_4 \\ 0 & -1 \end{bmatrix} \cdot \begin{bmatrix} 1 & T_1 \\ 0 & 1 \end{bmatrix} \cdot \begin{bmatrix} 1 & 0 \\ -\frac{1}{f_1} & 1 \end{bmatrix} \quad (9)$$

$f_1$ ,  $f_2$  denote the focal lengths of the lenses and  $T_1$ ,  $T_2$  and  $T_3$  are translation vectors, respectively.

It has to be mentioned that the matrix method treats light propagation ideally. As a consequence, focusing of a laser beam causes a spot with radius 0 in matrix description. To overcome such an obvious shortcoming, a complex beam parameter can be defined which allows treatment of laser beams in a more realistic way by means of the matrix method [8]. Since we are dealing with multiple reflections to achieve a more or less homogenous intensity distribution with dimensions much larger as the focal spot we can safely omit the complex treatment.

With the description above we can describe the properties of a laser beam after propagation through a kaleidoscope, with and without focusing lenses. As can be seen from the description of kaleidoscope transfer matrix, the quality of the beam homogenization depends on the term  $l_1 - l_4$ , which in turn depends on the relation between length  $L$  and opening width  $d$  of the kaleidoscope and incoming beam parameters. An incoming laser beam is focused into the opening of the homogenizer. Due to multiple reflections inside the kaleidoscope, the output intensity is nearly "flat-top". If we define the quality of the homogenization as the relation between the intensity near the "edge" and the centre of the beam, we are able to determine the minimal length of a kaleidoscope for any given opening width and beam parameters for a desired homogenization. Due to the divergence of the beam, the output opening has to be projected onto the surface of a sample by means of a focusing lens. From the considerations above it is clear that multiple reflections inside the kaleidoscope are responsible for homogenization. If we assume a reflectivity of 97.5%, losses summarize up to approximately 10% after 4 reflections inside the homogenizer which emphasizes the necessity of adequate cooling.

The radius of a laser beam with a Gaussian intensity distribution is defined as the distance from the axis where the intensity drops to  $1/e^2$  of the on-axis intensity. If we apply a similar criterion for the quality of our beam homogenizer we can determine from (fig.3) a minimum length of approx. 16  $d$ . As can be seen from Figure 2, the ratio between intensity at the edge and the center of the

beam increases for an increasing L/d ratio. If we take into account that the simplification treats only a 2-dimensional problem and that we neglected beam losses due to absorption, we can propose an optimum L/d ratio of approx. 25.

## 5. RESULTS

For better comparability results refer to the energy input per length. Such a line energy contains information about the optical power as well as the propagation speed. The resulting moldings are characterised by the ablation depth and width. An approximated area cross-section in form of a rectangular has been calculated with these values. It has to be mentioned that this area of cross section contains an error, since the shape of the real cross-section is smaller than the calculated area. Moreover, results achieved with the beam homogenization are better approximated by a rectangular shape as the results of the experiments which have been performed with the 200 mm focal length lens. The values are therefore not comparable with each other. Depth and width have been measured at the centre of the processed track to ensure that the process was steady state.

### 5.1. Experiments with a focal length of 200 mm

The experiments show that it is possible to ablate the desired volume in reasonable time. Unfortunately, results indicate that it is not possible to produce a box-shaped profile with this setup. The resulting cross section is more or less V-shaped. Figure 6 shows the cross section of a sample with the measured rectangular.

It can also be observed that the optical energy needed to evaporate a certain volume is higher than expected. The difference is that high, that it is not possible to explain the differences by a somewhat lower absorption coefficient or slightly different thermodynamic properties of materials used for experiments.

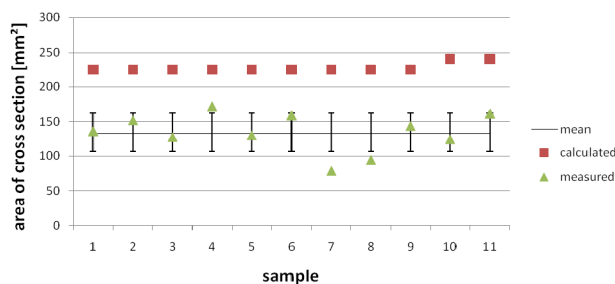


Figure 3: Comparison between measured and calculated area of cross section, line energy 9 J/mm, 30 l/min gas flow

The following figure 4 shows measured and calculated values of the cross section at an energy input per unit length of 9 J/mm, but with a different gas flow rate of 50 l/min.

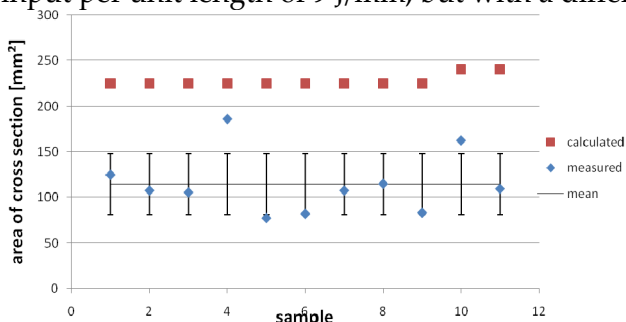


Figure 4: Comparison between measured and calculated area of cross section for a gas flow of 50 l/min, line energy 9 J/mm

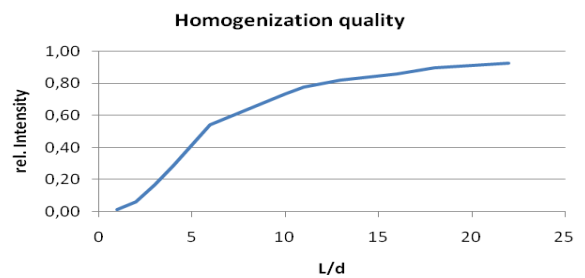


Figure 2: Relative intensity between the edge and the center of a beam at the output plane of a kaleidoscope with L length and d opening width

Figure 3 shows a comparison between calculated values for the area of cross section and measured values. All samples have been processed with the same energy input and gas flow (9 J/sample, 30 l/min). The ratio between mean value of the measured area and the calculated values is about 0.6.

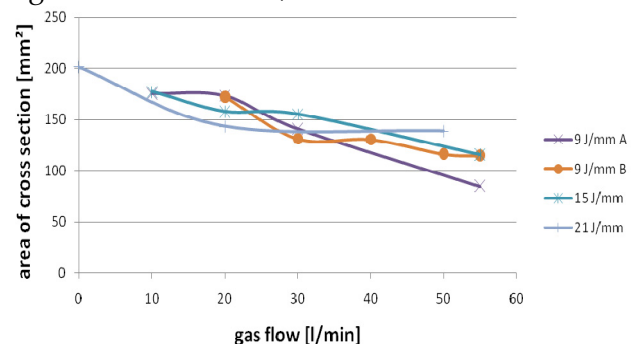


Figure 5: Area of cross section in dependency of gas flow rate

Measured values again differ from the calculated values with a larger variance. The ratio between mean of the measured areas and the calculated values is about 0.5.

It seems that for stronger gas flow more optical power is needed to evaporate a certain area. Figure 5 gives a detailed view on this behaviour. The measured area of cross section is drawn against the gas volume flow for different energy inputs per unit length. Despite the fact that the overall number of valid experiments is relatively low and graphs differ, it is obvious that an increasing gas flow results in a smaller area of cross section.

## 5.2. Experiments with beam homogenization

The produced mouldings approximate a box-shaped profile considerably better than the results without homogenization, even though there is still room for improvement. Evaporated volume increased, too.

As already mentioned values from this series of tests cannot be compared with the previous series, as the shape of the moulding is different and therefore the error of the calculated area of the cross-section is different. Figure 8 and figure 9 show the calculated and measured areas of cross section for 48 J/mm and 24 J/mm, respectively. Again, results indicate that material removal rate decreases with increasing gas pressure.

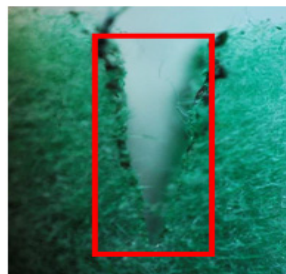


Figure 6: Evaporated area with rectangular shaped area used for calculation of a sample from first series

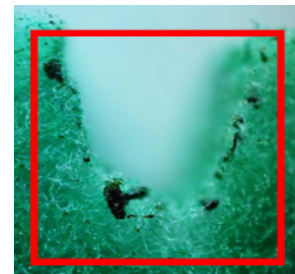


Figure 7: Evaporated area with measured rectangular, homogenized laser beam

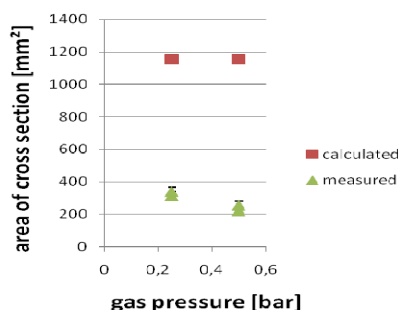


Figure 8: Area of cross section, 48 J/mm

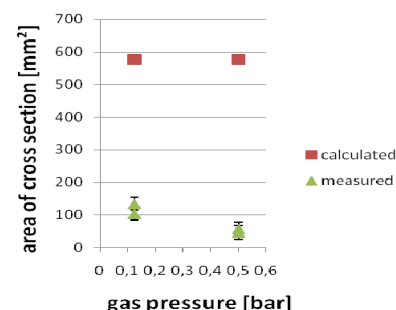


Figure 9: Area of cross section, 24 J/mm

## 6. DISCUSSION AND OUTLOOK

Presented results show that it is possible to produce moldings into non-woven fabrics by laser ablation. Due to the thermal nature of CO<sub>2</sub>-laser processing it was not possible to avoid droplet formation totally. Additionally, the shape of the moldings has been improved by beam homogenization but suffers still from irregularities from the desired box-shaped profiles.

A procedure to achieve a uniform intensity distribution by means of a kaleidoscope and a criterion for the quality of the homogenizer was presented. Results confirm that beam homogenization improves the shape of the moldings in comparison to a lens with a long focal length. Calculated energy required for removal of a certain amount of material differs from measured values strongly. It has been assumed that the differences result from the gas flow but a satisfying explanation is still missing. Further work has to be done to determine this effect completely. To improve the shape of the moldings more attention has to be paid on the gas flow. For example, influences of a coaxial gas supply, a (coaxial) suction as well as the use of different gases should be examined.

## 7. REFERENCES

- [1.] Eyerer, P., Hirth, T., Elsner, P.: Polymer Engineering, Springer, Berlin, 2007.
- [2.] Weigand, E.: Recycling und Verwertung von Polyurethanen, [http://www.pur.bayer.com/BMS/PUR-Internet.nsf/files/polyurethanes/\\$file/5605489\\_d.pdf](http://www.pur.bayer.com/BMS/PUR-Internet.nsf/files/polyurethanes/$file/5605489_d.pdf), 2013-04-11.
- [3.] Directive 2000/53/EC of the European Parliament and of the Council, 2000.
- [4.] Bäuerle, D.: Laser processing and chemistry, 2nd ed., Berlin, Springer, New York, 1996.
- [5.] Schüöcker, D.: Handbook of Eurolaser Academy, Vol. 2, Chapman & Hall, 1998.
- [6.] Kroschwitz, J.I.: Encyclopedia of Polymer Science and Engineering, John Wiley & Sons, 1988.
- [7.] Schüöcker, D.: Handbook of Eurolaser Academy, Vol. 1, Chapman & Hall, 1998.
- [8.] Gerrard, A., Burch, J.M.: Introduction to matrix methods in optics, Dover Publications, New York, 1994.